HHS Public Access

Author manuscript

ACS Chem Biol. Author manuscript; available in PMC 2019 October 10.

Published in final edited form as:

ACS Chem Biol. 2016 August 19; 11(8): 2124–2130. doi:10.1021/acschembio.6b00447.

Mapping the Trimethoprim-Induced Secondary Metabolome of *Burkholderia thailandensis*

Bethany K. Okada[†,#], **Yihan Wu**[†,#], **Dainan Mao**[†], **Leah B. Bushin**[†], **Mohammad R. Seyedsayamdost**[†,‡,*]

[†]Department of Chemistry, Princeton University, Princeton, NJ 08544

[‡]Department of Molecular Biology, Princeton University, Princeton, NJ 08544

Abstract

While bacterial genomes typically contain numerous secondary metabolite biosynthetic gene clusters, only a small fraction of these are expressed at any given time. The remaining majority is inactive or silent, and methods that awaken them would greatly expand our repertoire of bioactive molecules. We recently devised a new approach for identifying inducers of silent gene clusters and proposed that the clinical antibiotic trimethoprim acted as a global activator of secondary metabolism in *Burkholderia thailandensis.* Herein we report that trimethoprim triggers the production of over 100 compounds that are not observed under standard growth conditions, thus drastically modulating the secondary metabolic output of *B. thailandensis.* Using MS/MS networking and NMR, we assign structures to ~40 compounds, including a group of new molecules, which we call acybolins. With methods at hand for activation of silent gene clusters and rapid identification of small molecules, the hidden secondary metabolomes of bacteria can be interrogated.

The emergence of mass spectrometry-based ‘omics approaches has revolutionized our understanding of metabolism. Work over the last century combined with recent technological advances has led to a detailed, comprehensive, and quantitative picture of primary metabolism. This kind of understanding, however, is not yet available for secondary metabolism. We do not know how vast it is; a global picture of the total secondary metabolome is not yet available for any given bacterium.[1] With recent developments in mind, one may begin to ask whether this kind of insight can be attained, and a comparison with primary metabolism reveals the challenges in doing so: First, primary metabolism is essential for growth and proliferation and consequently the metabolic enzymes are always expressed, some at very high intracellular concentrations. This is not the case for secondary

[*]**Corresponding Author** mrseyed@princeton.edu.

Author Contributions

[#](B.K.O., Y.W.) These authors contributed equally to this work.

Associated Content

Materials and Methods; 1D/2D NMR spectra for **19**–**21** and **29**–**33**, HR-MS data for **1**–**40**, fragmentation patterns of HAQs, HR-MS/MS data for HAQs (**3**, **9**–**18**) bactobolin I (**22**) and acybolins (**29**–**37**), Marfey’s analysis for **29**; Mosher ester analysis for **29**; HPLC-MS analysis of mutant *ΔbtaQ* for production of acybolins. This material is available free of charge via the Internet at http://pubs.acs.org.

The authors declare no competing financial interests.

metabolism, where most biosynthetic pathways are not actively expressed when bacteria are cultured under normal growth conditions. These pathways are referred to as 'cryptic' or 'silent', and activating the corresponding biosynthetic gene clusters is an important area of active research.[2] Second, primary metabolism is target-oriented and converges to a few known end products. This complex network of interrelated structures facilitates isotopic tracer experiments and identification of intermediates. Secondary metabolism, on the other hand, is diversity-oriented and diverges into many unknown end products. Within a bacterial host, these pathways are for the most part unrelated to one another.[3] To address these challenges and illustrate the total secondary metabolic capability of a given bacterium, methods need to be developed that activate silent biosynthetic pathways and allow for rapid structural elucidation of large numbers of divergent secondary metabolites. Herein, we work toward this goal and combine methods for inducing silent gene clusters, using small molecule modulators, with untargeted metabolomics and mass spectral networking to provide a snapshot of the silent secondary metabolome of *Burkholderia thailandensis* E264.

We recently developed a method for finding elicitors of silent biosynthetic gene clusters.[4] When applied to the cryptic *mal* gene cluster in *B. thailandensis* E264 (hereafter E264), which produces the virulence factor malleilactone,[5,6] the antibiotic trimethoprim (Tmp), at sub-lethal concentrations, was revealed as the most potent inducer among a family of 640 candidates tested. Aside from a ~140-fold overproduction of malleilactone, we also observed that a number of other biosynthetic pathways were activated by Tmp, perhaps suggesting that it had cell-wide induction effects on secondary metabolism. To examine this idea further, we have utilized a suite of metabolomics and spectral networking analyses that have helped us gauge the influence of Tmp on the secreted metabolome of E264. Our workflow started by generating triplicate Tmp-induced and uninduced E264 cultures and isolating the secreted metabolites by three complementary chemical extraction methods. The resulting extracts were subjected to HPLC-Qtof-MS analysis. Untargeted molecular feature extraction in the Tmp-induced samples, compared to the control (no Tmp), qualitatively shows significant induction of a large number of metabolites (Fig. 1). Metabolomic analysis showed that >100 compounds were induced by sub-lethal levels of Tmp (see SI). These effectively represent the Tmp-induced metabolome, likely consisting of known compounds, analogs of known compounds, and cryptic metabolites. This analysis confirms that Tmp does indeed considerably induce secondary metabolism in *B. thailandensis* E264.

Given the ~22 biosynthetic gene clusters of E264,[7] it was surprising to find >100 secreted metabolites in response to Tmp. To shed light on this issue, we set out to identify the compounds induced by Tmp. It would be an arduous task to isolate >100 compounds and solve their structures individually. Instead, in an effort to simplify this process, we opted to use mass spectral networking to organize the Tmp-induced metabolites by their MS/MS fragment ions, which serves as an indicator of structural relatedness. This method has recently been pioneered by the Dorrestein group and has deeply impacted natural products discovery.[8,9] Several untargeted Qtof-MS/MS runs with varying collision energies were carried out on both Tmp-induced and uninduced samples and the resulting spectra were organized in a molecular network (Fig. 2A). In this network, each node corresponds to a distinct metabolite, while the lines connecting the nodes are indicators of the structural similarity between these compounds. The thicker the line, the more MS/MS fragment ions

are shared by the two corresponding nodes. The Tmp-induced metabolites are shown in blue, those unique to the uninduced sample in orange, and metabolites common to both samples in green. This latter group consists mostly of metabolites that were generated in the absence of Tmp but were significantly upregulated in its presence. By organizing a group of ~240 compounds into 14 large molecular families, this analysis significantly simplifies the task of assigning the Tmp-induced metabolome. It further prioritizes discovery efforts to find new and cryptic metabolites.

To analyze the molecular network, we began by assigning compound clusters of known metabolites. The high-resolution (HR)-MS and MS/MS data helped identify clusters of compounds related to bactobolin (**1**),[10,11] the lasso peptide capistruin (**2**),[12] 4-hydroxy-3-methyl-2-nonenylquinoline (HMNQ, **3**),[13] burkholdac (**4**),[14–16] terphenyl (**5**),[17] malleilactone (**6**),[5,6] trimethoprim and its metabolized products (**7**) and the polyene thailandamide (**8**) (Fig. 2A, Table S1).[18] Aside from identifying them, the network also allowed us to assign specific molecules to many nodes using the HR-MS/MS data. In the case of the quinolines, we were able to assign structures to 11 nodes, consistent with previous reports that E264 generates a family of such metabolites (Fig. 2B, **3**, **9–18**).[13] Members of this family vary in the length and saturation of the 2-alkyl substituent, as well as the presence of an N-oxide and a 3-methyl substituent (Fig. S1, Table S2). We observed the 4-hydroxy-3-methylquinolines **14** and **18** only in the presence of Tmp, quinoline **17** only in its absence, while the remaining derivatives were seen under both conditions. Compounds **13**, **14**, and **17** are new to E264, while the other quinolines have been reported before.[13]

A similar analysis was carried out with the capistruin molecular family. Capistruin A (**2**) was a cryptic metabolite, but heterologous expression in *E. coli* and growth of E264 at 42°C allowed Marahiel and colleagues to identify the product of this gene cluster.[12] In our case, Tmp acts as an efficient activator of the silent capistruin gene cluster. We identified the parent capistruin, as previously reported, but also found two analogs (**19** and **20**), produced only in the presence of Tmp, lacking either the *C*-terminal residue or the last two *C*-terminal residues compared to capistruin (Fig. 2C, Table S3–S4). To ensure that they were indeed lasso peptides, we isolated the two analogs and generated 3D structural models using NMR NOESY constraints and the CYANA algorithm (Table S5).[19] The data clearly indicate the presence of a lasso motif and suggest that E264, in the presence of Tmp, can generate a library of capistruin analogs probably mediated by a carboxypeptidase-like protease that removes amino acid residues from the *C*-terminal end of the peptide (Fig. 2C). Whether this occurs before or after lasso motif formation is presently unknown. In a similar fashion, we were able to identify a new thailandamide analog, a geometric isomer of the previously reported thailandamide A (**21**, Fig. S2–S3, Table S6) as well as a new bactobolin analog (**22**, Fig. S4, see below). A number of previously described compounds, including bactobolins (**23–26**), malleilactone B (**27**), and burkholdac A (**28**) were also identified (Fig. S2). In sum, the molecular network allowed us to rapidly assign structures to 28 compounds – of these, 7 represent new analogs of previously reported molecules.

The strength of the differential molecular network above is not merely finding new analogs, but rather helping identify cryptic ones that are induced by Tmp, and we consequently turned our focus to these metabolites. Among them, we were intrigued by two clusters of

high MW compounds (Fig. 2A, shadowed pink clusters). One of these appeared to be related to bactobolins as judged by the dichloro MS pattern, while the other did not show any significant relation to other metabolites. We tackled the former first. As elaborated in Fig. S5, these compounds, which we call acybolins, are indeed cryptic metabolites produced upon Tmp treatment, but not under normal growth conditions. To examine the detailed structure of acybolins, large-scale production cultures of E264 were prepared in the presence of Tmp. UV- and mass-guided isolation using a series of liquid- and solid-phase extractions followed by HPLC purification yielded 5 analogs with yields of 0.08–0.4 mg/L culture (**29**–**33**). A panel of 1D and 2D NMR spectra was analyzed to elucidate the structures of acybolins (Figure 3, Fig. S6–S11, Table S7–S12). Assessment of ^{1}H and TOCSY NMR spectra revealed two spin systems separated by a peptidic linker consisting of the sequence Ala-Ala-Ala-Gly in the most abundant analog, acybolin A (**29**, Fig. 3A). One spin system was identified as a 3-hydroxydecanoyl group. HMBC correlations from the glycine α-protons at 3.94 and 3.80 ppm to C17’ at 175.2 ppm showed that the acyl group was attached to the *N*-terminal Gly of the peptide linker (Figure 3A, B). In the second spin system, a characteristic singlet at 6.29 ppm was assigned to the ^{1}H adjacent to a dichloro group and further analysis by COSY, HSQC, and HMBC spectra identified the second spin system as the bactobolin bicycle. HMBC correlations from C4 at 4.65 ppm to the carbonyl-C2’ at 175.5 ppm indicated that the bicycle was connected to the *C*-terminal end of the peptide linker and completed the structural assignment. Marfey’s analysis[20] with acybolin A indicated that all Ala residues were in the L-configuration (Fig. S12). Mosher ester analysis[21] revealed the R stereoconfiguration for the hydroxyl group on the acyl side chain (Fig. S13).

Further compelling support for the structure of acybolins was garnered by HR-MS and tandem HR-MS. The former gave $[M+H]^+$ of 736.3094, consistent with a molecular formula of $C_{32}H_{51}O_{10}N_5Cl_2$ ($[M+H]^+_{calc}$ 736.3091, Table S12), while the latter allowed identification of the acylated b1, b2, and b3 ions as well as the bactobolin-bearing y1, y2, y3, and y4 ions. Similar fragmentations were observed with acybolins B-E (Table S13). With these at hand, the structures of four additional analogs were elucidated unambiguously by HR-MS/MS analysis (**34**–**37**, Figure 3C, Table S13). These nine analogs contain the same acyl chain as acybolin A but vary in the sequence and length of the peptide linker as well as the presence of an OH group at C5 in the bactobolin heterocycle. Collectively, the NMR and HR-MS data support our assignment of the acybolin structures as hybrid molecules containing the bactobolin bicycle and a tri-, tetra-, or pentapeptide linker acylated with a 3-hydroxydecanoyl chain.

B. thailandensis E264 harbors three quorum sensing (QS) systems consisting of the LuxI/LuxR pairs of BtaI1-BtaR1, BtaI2-BtaR2, and BtaI3-BtaR3.[22–24] These generate and respond to the acyl homoserine lactone (AHL) signals shown (Figure 4A). Acybolins are bivalent molecules, part antibiotic, part signaling agent, as they appear to incorporate the acyl chain of a QS signal, generated by BtaI2, with an antibiotic warhead, the bactobolin scaffold. Interestingly, the bactobolin gene cluster (*bta*) harbors the *btaI2* gene in the middle of the cluster, several genes separated from its cognate *btaR2* response regulator (Figure 4B). This is in contrast to the canonical arrangement of *luxI-luxR* pairs, which are usually

adjacent to one another and not embedded inside another biosynthetic gene cluster.[25,26] Aside from BtaI2, a second ligase is encoded by BtaQ with an unknown function (Figure 4B). To identify the gene cluster responsible for acybolin production, we assessed several gene deletion mutants. We began by testing a bactobolin-deficient mutant carrying a transposon insertion in *btaK* (*btaK::Tn*)[27] for its ability to synthesize acybolin. In the presence and absence of Tmp, the *btaK* mutant failed to generate any of the acybolin analogs consistent with the involvement of the *bta* cluster in biosynthesizing this family of compounds (Fig. 4C).

The role of *btaQ* was examined by generating a markerless deletion mutant using established genetic methods (Table S14).[28] This mutant, however, was able to synthesize acybolins in response to Tmp (Fig. S14). We next assessed involvement of the remaining ligase in the *bta* cluster, BtaI2. Because the three LuxI enzymes in E264 have overlapping specificities (Figure 4A), we assessed a triple mutant containing a markerless deletion in all three *luxI* genes (*ΔbtaI1/I2/I3*).[24] As expected, this mutant failed to synthesize any of the AHLs. In response to Tmp and either 3-OH-C_8-HSL or 3-OH-C_{10}-HSL, it did however synthesize acybolins (Fig. 4D). These results indicate that the ligase is not provided by any genes inside the *bta* cluster, but that its expression is dependent on the presence of the antibiotic stressor Tmp. While the identity of the acybolin ligase requires further studies, the results indicate that diffusible small molecule signals can modulate the output of the *bta* cluster. AHL-mediated quorum sensing gives rise to bactobolin while a combination of AHLs and Tmp elicits production of the cryptic acybolins.

With the acybolin MS/MS cluster identified, we next focused on the other Tmp-induced molecular family in the network and isolated and structurally elucidated the most abundant member within this group using NMR (**38**, Fig. 2A). This compound turned out to be a linear peptide with the sequence shown; it exhibited no useful bioactivity when tested in growth inhibition assays against *E. coli* and *B. subtilis.* A large cluster in the MS/MS network similarly appears to consist of peptide fragments. HR-MS/MS allowed identification of a number of these fragments, two of which is shown (**39** & **40**, Fig. 2A). Together with the modifications found in capistruins B and C and the presence of compounds **38**–**40** suggests that Tmp induces production of extracellular proteases, which modify existing secondary metabolites and other peptides present in the medium. It has been shown that Pseudomonads produce a number of extracellular proteases as virulence factors.[29,30] Such proteases may also be produced by *B. thailandensis* in response to Tmp; this would indicate that a complete picture of the secreted metabolome of E264 needs to include extracellular proteases, which may only be expressed under certain conditions.

In this study we have addressed two key challenges in natural products discovery: activation of silent biosynthetic gene clusters and rapid assignment of structurally divergent secondary metabolites. By combining small molecule elicitation with metabolomic analyses, we show that *B. thailandensis* E264 synthesizes a spectacular array of diverse, complex secondary metabolites, especially when challenged by Tmp. Mass spectral networking allowed us to rapidly identify 40 metabolites, including analogs of known compounds and the acybolins, a family of bivalent, cryptic metabolites. The combination used herein facilitates natural products discovery by eliciting hidden metabolites and at the same time provides a means of

dereplication and thus prioritization in the search for new metabolites. Future applications of this combination promise to reveal a global picture of the secondary metabolomes of bacteria. They will also address the mechanism of induction by exogenous elicitors, such as Tmp.

Methods

A description of materials used, generation of mutant strains, structural elucidation of acybolins, metabolomic analysis, generation of MS/MS network, and other protocols is given in the SI.

General procedures.

HPLC separations were carried out on an Agilent 1260 Infinity Series analytical or preparative HPLC system equipped with a photodiode array detector and an automated fraction collector. Low resolution HPLC-MS analysis was performed on an Agilent instrument consisting of an automated liquid autosampler, a 1260 Infinity Series HPLC system coupled to a photodiode array detector and a 6120 Series ESI mass spectrometer. A Phenomenex Luna C18 column (5 μm, 4.6 × 100 mm) was used with a flow of 0.6 mL/min and a gradient of 20% MeCN in H_2O to 100% MeCN (+0.1% (v/v) formic acid). High-resolution (HR) HPLC-MS and HR-tandem HPLC-MS were carried out on an Agilent UHD Accurate Mass Qtof LC-MS system, equipped with a 1260 Infinity Series HPLC, an automated liquid sampler, a photodiode array detector, a JetStream ESI source, and the 6540 Series Qtof. For routine analysis, samples were separated on an Agilent Poroshell 120 EC-C18 column (2.7 μm, 3 × 50 mm) operating at 0.4 mL/min with a gradient of 20% MeCN in H_2O to 100% MeCN (+0.1% (v/v) formic acid) over 13 min. NMR spectra were acquired at the Princeton University Department of Chemistry NMR Facilities. Spectra were collected in MeOD-*d4* in the triple resonance cryoprobe of a Bruker A8 Avance III HD 800 MHz NMR spectrometer.

Purification of acybolins.

Wt *B. thailandensis* E264 grown on an LB agar plate was used to inoculate 5 mL of LB medium in a 14 mL sterile culture tube. After overnight growth at 30°C and 250 rpm, the culture was diluted to an $OD_{600\ nm}$ of 0.05 into 50 mL of LB in a 250 mL Erlenmeyer flask. This culture was grown overnight at 30°C and 250 rpm and used to inoculate 650 mL LB-Mops (LB + 50 mM Mops, pH 7) in each of 12 × 4 L Erlenmeyer flasks. The initial $OD_{600\ nm}$ of the large cultures was 0.05 and the cultures contained 30 μM trimethoprim, prepared as a 10 mM stock in DMSO. After 26 h growth at 30°C and 200 rpm, the cultures were extracted twice with one volume of EtOAc. The organic layers were combined, dried over Na_2SO_4, and evaporated completely in vacuo. The remaining residue was resolved by solid-phase extraction using a 10 g Seppak-C18 column, which had been washed with MeCN and equilibrated with 15% MeCN in H_2O. Step-wise elution was performed with 100 mL of 15%, 35%, 55%, 75%, and 100% MeCN (in H_2O), all containing 0.1% formic acid. The 55% MeCN fraction contained the desired acybolins. These were further purified on a manual Hypercarb column (Fisher Scientific), which had been equilibrated with 20% MeCN in H_2O. Step-wise elution was performed with 15 mL of 20%, 35%, 50%, 75%, and 100%

MeCN (in H_2O+0.1% (v/v) formic acid). The 35% and 50% MeCN fractions were combined, dried in vacuo, resuspended in MeOH, and purified by reverse-phase HPLC on a preparative Eclipse XDB-C8 column (Agilent, 7 μm, 21.2 × 250 mm) operating at 12 mL/min. The elution program started with an isocratic step (5 min, 20% MeCN in H_2O), followed by a gradient from 20–100% MeCN (+0.1% formic acid) over 30 min. The desired acybolins eluted at ~62–68% MeCN, and fractions containing acybolins were combined, dried in vacuo, and further purified by reverse-phase HPLC on a preparative Luna C18 column (Phenomenex, 5 μm, 21.2 × 250 mm) operating at 12 mL/min. The elution program included an isocratic step (30 min, 30% MeCN in H_2O), followed by a gradient from 30–100% MeCN (+0.1% formic acid) over 20 min. The desired acybolins eluted at ~74–80% MeCN. Fractions containing acybolins were combined and further purified by reverse-phase HPLC on an analytical Synergi Fusion-RP column (Phenomenex, 4 μm, 4.6 × 250 mm) operating at 1 mL/min. Acybolins were eluted isocratically at 32% MeCN in H_2O (+0.1% formic acid) over 50 min. The acybolins eluted in separate fractions between 33 and 46 minutes, yielding 0.6–3 mg of pure material.

Supplementary Material

Refer to Web version on PubMed Central for supplementary material.

Acknowledgements

We thank J. Chandler for the kind gift of the triple *btal* mutant, J. Blodgett for the kind gift of *E. coli* JV36, K. Davis for assistance with figures 1 & 2, and the Searle Scholars Program of the Kinship Foundation (to M.R.S) for generous support of this work.

References

(1). Nett M., Ikeda H., and Moore BS (2009) Genomic basis for natural product biosynthetic diversity in the actinomycetes. Nat. Prod. Rep. 26, 1362–1384 [PubMed: 19844637]

(2). Rutledge PJ, and Challis GL (2015) Discovery of microbial natural products by activation of silent biosynthetic gene clusters. Nat. Rev. Microbiol. 13, 509–523. [PubMed: 26119570]

(3). Fischbach MA, and Walsh CT (2006) Assembly-line enzymology for polyketide and nonribosomal peptide antibiotics: logic, machinery, and mechanisms. Chem. Rev. 106, 3468–3496. [PubMed: 16895337]

(4). Seyedsayamdost MR (2014) High-throughput platform for the discovery of elicitors of silent bacterial gene clusters. Proc. Natl. Acad. Sci. USA 111, 7266–7271. [PubMed: 24808135]

(5). Biggins JB, Ternei MA, and Brady SF (2012) Malleilactone, a polyketide synthase-derived virulence factor encoded by the cryptic secondary metabolome of Burkholderia pseudomallei group pathogens. J. Am. Chem. Soc. 134, 13192–13195. [PubMed: 22765305]

(6). Franke J., Ishida K., and Hertweck C. (2012) Genomics-driven discovery of burkholderic acid, a noncanonical, cryptic polyketide from human pathogenic Burkholderia species. Angew. Chem. Int. Ed. Eng. 51, 11611–11615.

(7). Liu X., and Cheng Y-Q (2014) Genome-guided discovery of diverse natural products from Burkholderia sp. J. Ind. Microbiol. Biotechnol. 41, 275–284. [PubMed: 24212473]

(8). Watrous J., Roach P., Alexandrov T., Heath BS, Yang JY, Kersten RD, van der Voort M., Pogliano K., Gross H., Raaijmakers JM, Moore BS, Laskin J., Bandeira N., and Dorrestein PC (2012) Mass spectral molecular networking of living microbial colonies. Proc. Natl. Acad. Sci. USA 109, E1743–E1752. [PubMed: 22586093]

(9). Bouslimani A., Sanchez LM, Garg N., and Dorrestein PC (2014) Mass spectrometry of natural products: current, emerging and future technologies. Nat. Prod. Rep. 31, 718–729. [PubMed: 24801551]

(10). Seyedsayamdost MR, Chandler JR, Blodgett JAV, Lima PS, Duerkop BA, Oinuma K, Greenberg EP, and Clardy J. (2010) Quorum-sensing-regulated bactobolin production by Burkholderia thailandensis E264. Org. Lett.12, 716–719. [PubMed: 20095633]

(11). Kondo S, Horiuchi Y, Hamada M, Takeuchi T, and Umezawa H. (1979) A new antitumor antibiotic, bactobolin produced by Pseudomonas. J. Antibiot. 32, 1069–1071. [PubMed: 528370]

(12). Knappe TA, Linne U, Zirah S, Rebuffat S, Xie X, and Marahiel MA (2008) Isolation and structural characterization of capistruin, a lasso peptide predicted from the genome sequence of Burkholderia thailandensis E264. J. Am. Chem. Soc. 130, 11446–11454. [PubMed: 18671394]

(13). Vial L, Lepine F, Milot S, Groleau M-C, Dekimpe V, Woods DE, and Deziel E. (2008) Burkholderia pseudomallei, B. thailandensis, and B. ambifaria produce 4-hydroxy-2-alkylquinoline analogues with a methyl group at the 3 position that is required for quorum-sensing regulation. J. Bacteriol. 190, 5339–5352. [PubMed: 18539738]

(14). Biggins JB, Gleber CD, and Brady SF (2011) Acyldepsipeptide HDAC inhibitor production induced in Burkholderia thailandensis. Org. Lett. 13, 1536–1539. [PubMed: 21348454]

(15). Wang C, Henkes LM, Doughty LB, He M, Wang D, Meyer-Almes F-J, and Cheng Y-Q (2011) Thailandepsins: bacterial products with potent histone deacetylase inhibitory activities and broad-spectrum antiproliferative activities. J. Nat. Prod. 74, 2031–2038. [PubMed: 21793558]

(16). Benelkebir H, Donlevy AM, Packham G. and Ganesan A. (2011) Total synthesis and stereochemical assignment of burkholdac B, a depsipeptide HDAC inhibitor. Org. Lett. 13, 6334–6337. [PubMed: 22091906]

(17). Biggins JB, Liu X, Feng Z, and Brady SF (2011) Metabolites from the induced expression of cryptic single operons found in the genome of Burkholderia pseudomallei. J. Am. Chem. Soc. 133, 1638–1641. [PubMed: 21247113]

(18). Nguyen T, Ishida K, Jenke-Kodama H, Dittmann E, Gurgui C, Hochmuth T, Taudien S, Platzer M, Hertweck C, and Piel J. (2008) Exploiting the mosaic structure of trans-acyltransferase polyketide synthases for natural product discovery and pathway dissection. Nat. Biotechnol. 26, 225–233. [PubMed: 18223641]

(19). Güntert P, Mumenthaler C, and Wüthrich K. (1997) Torsion angle dynamics for NMR structure calculation with the new program DYANA. J. Mol. Biol. 273, 283–298. [PubMed: 9367762]

(20). Marfey P. (1984) Determination of D-amino acids. II. Use of a bifunctional reagent, 1,5-difluoro-2,4-dinitrobenzene. Carlsberg Res. Commun. 49, 591–596.

(21). Hoye TR, Jeffrey CS, and Shao F. (2007) Mosher ester analysis for the determination of absolute configuration of stereogenic (chiral) carbinol carbons. Nat. Protocol. 2, 2451–2458.

(22). Majerczyk C, Brittnacher M, Jacobs M, Armour CD, Radey M, Schneider E, Phattarasokul S, Bunt R, and Greenberg EP (2014) Global analysis of the Burkholderia thailandensis quorum sensing-controlled regulon. J. Bacteriol. 196, 1412–1424. [PubMed: 24464461]

(23). Duerkop BA, Varga J, Chandler JR, Peterson SB, Herman JP, Churchill MEA, Parsek MR, Nierman WC, and Greenberg EP (2009) Quorum-Sensing control of antibiotic synthesis in Burkholderia thailandensis. J. Bacteriol. 191, 3909–3918. [PubMed: 19376863]

(24). Chandler JR, Duerkop BA, Hinz A, West TE, Herman JP, Churchill MEA, Skerrett SJ, and Greenberg EP (2009) Mutational analysis of Burkholderia thailandensis quorum sensing and self-aggregation. J. Bacteriol. 191, 5901–5909. [PubMed: 19648250]

(25). Ng W-L, and Bassler BL (2009) Bacterial quorum-sensing network architectures. Annu. Rev. Genet. 43, 197–222. [PubMed: 19686078]

(26). Schuster M, Sexton DJ, Diggle SP, and Greenberg EP (2013) Acyl-homoserine lactone quorum sensing: from evolution to application. Annu. Rev. Microbiol. 67, 43–63. [PubMed: 23682605]

(27). Gallagher LA, Ramage E, Patrapuvich R, Weiss E.; Brittnacher M, and Manoil C. (2013) Sequence-defined transposon mutant library of Burkholderia thailandensis. MBio. 4, e00604–13.

(28). Barrett AR, Kang Y, Inamasu KS, Son MS, Vukovich JM, and Hoang TT (2008) Genetic tools for allelic replacement of Burkholderia species. Appl. Environ. Microbiol. 74, 4498–4508. [PubMed: 18502918]

(29). Gambello MJ, Kaye S, and Iglewski BH (1993) LasR of Pseudomonas aeruginosa is a transcriptional activator of the alkaline protease gene (apr) and an enhancer of exotoxin A expression. Infect. Immun. 61, 1180–1184. [PubMed: 8454322]

(30). Smith RS, and Iglewski BH (2003) P. aeruginosa quorum-sensing systems and virulence. Curr. Opin. Microbiol. 6, 56–60. [PubMed: 12615220]

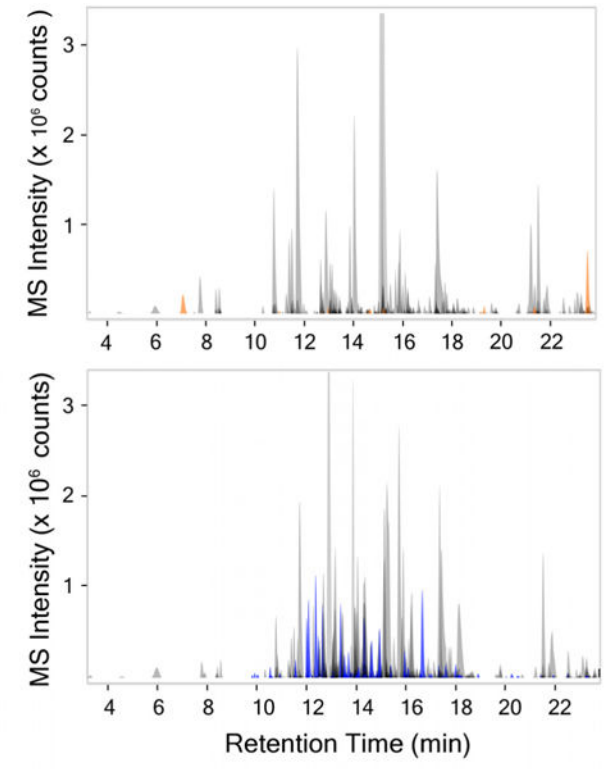

Figure 1.

Trimethoprim's effect on the secreted metabolome of E264. HPLC-Qtof-MS analysis of secondary metabolites produced in the absence (top) and presence of Tmp (bottom). Each peak corresponds to a unique compound or molecular feature, which has been mass-extracted and integrated. Features unique to the control (top) or Tmp sample (bottom) are shown in orange and blue, respectively (see SI).

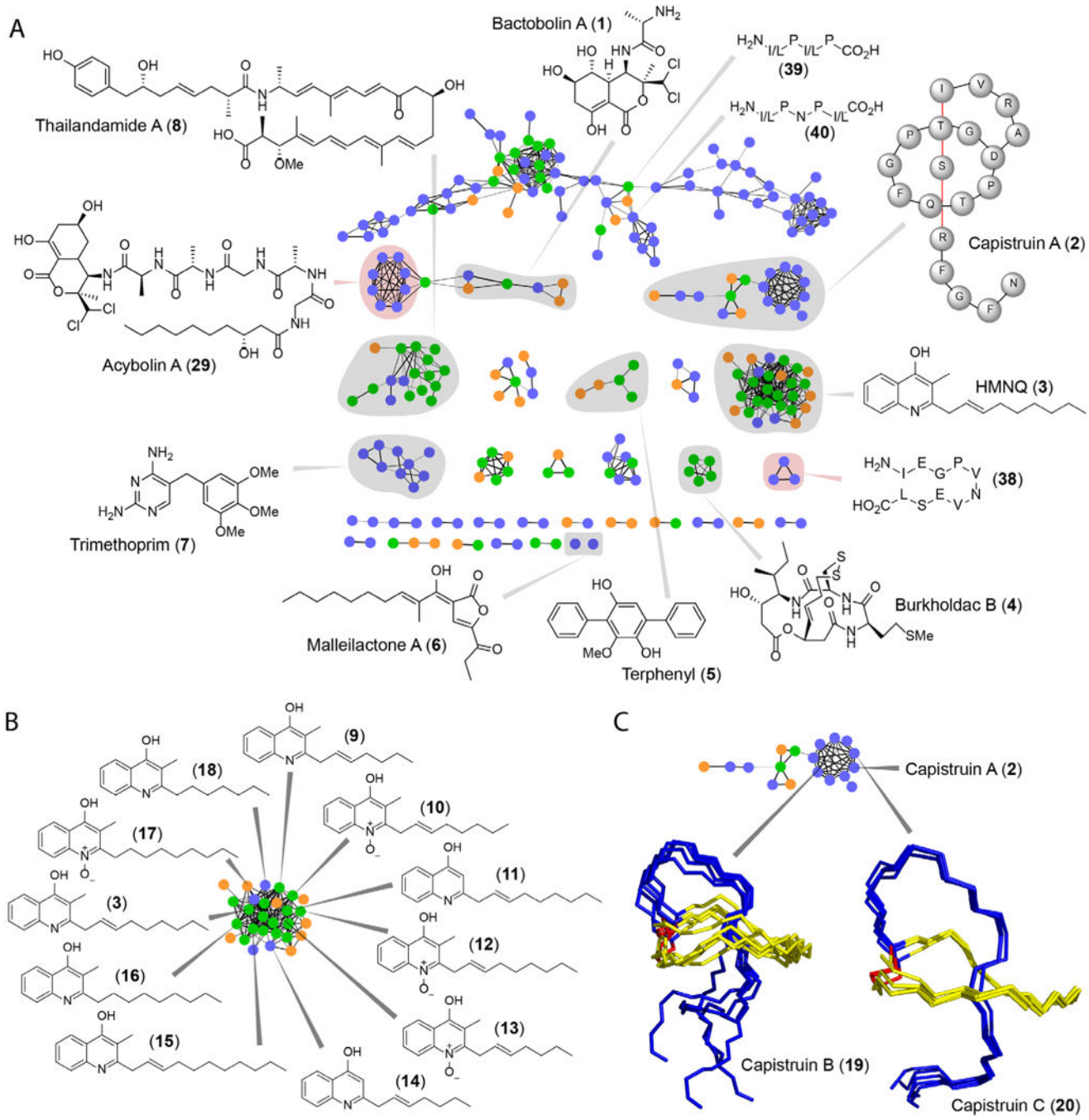

Figure 2.

The Tmp-Induced Metabolome of E264. (A) MS/MS network analysis of secreted metabolites by E264 in the presence of Tmp only (blue nodes), in the absence of Tmp (orange), or under both conditions (green). MS/MS clusters that were identified are shaded in gray and labeled. Clusters of cryptic metabolites examined further are shaded in pink. (B) Identification of HAQ congeners identified by HR-MS and tandem HR-MS. (C) New capistruin analogs (**19** and **20**) induced by Tmp. For both analogs, presence of the lasso

motif was confirmed by calculation of topological features using NMR NOESY constraints. The top 5 calculated conformers are superimposed for each analog.

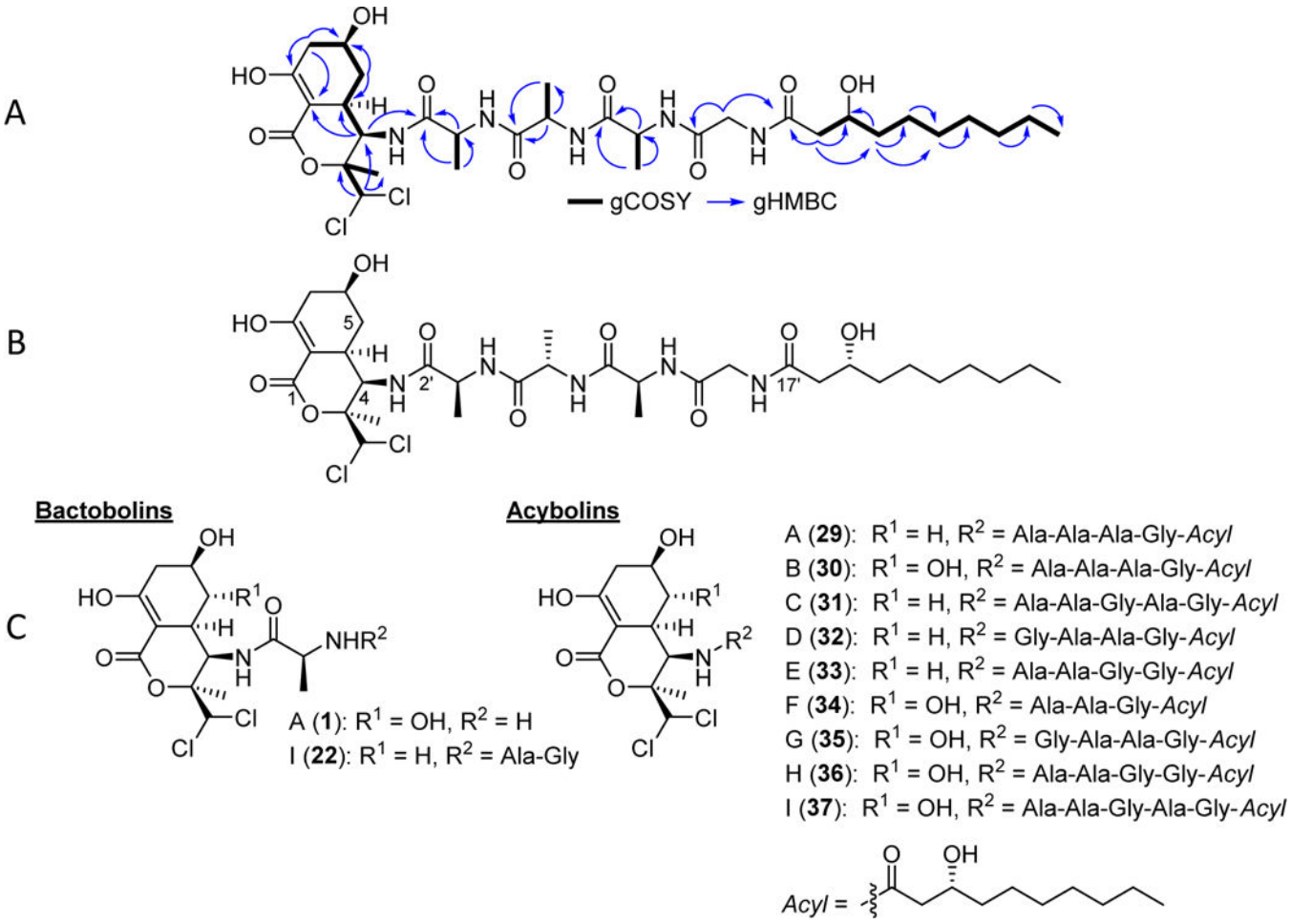

Figure 3.

Structural elucidation of acybolins. (A) Relevant gCOSY and gHMBC correlations used to solve the structure of acybolin A. (B) Structure of acybolin A; the stereochemistry of the Ala groups was determined to be L-Ala by Marfey's analysis. The R stereoconfiguration was determined for the hydroxyl group on the acyl substituent using Mosher ester analysis. (C) Structures of acybolins A–I and bactobolins A and I. Acybolins A–I and bactobolin I were isolated and structurally elucidated in this study.

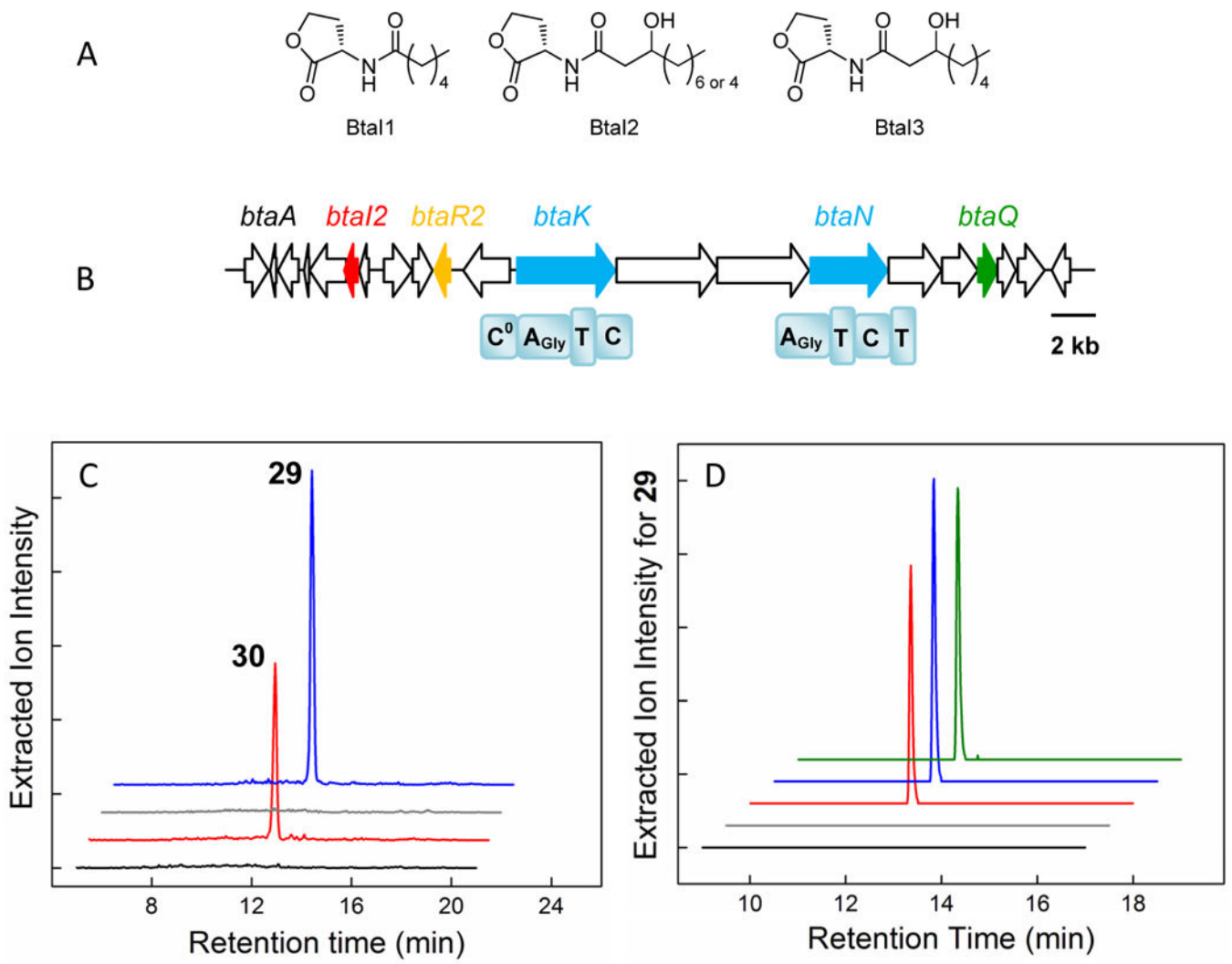

Figure 4.

Modulation of the products of the *bta* cluster by small molecules. (A) Products of the three AHL synthases in E264 generated from *S*-adenosylmethionine and varying acyl groups. Acybolin contains the same acyl chain as the product of BtaI2, which is encoded in the bactobolin gene cluster. (B) The *bta* gene cluster on chromosome II of E264, as previously annotated. *BtaQ* (green), *btaI2* (red) and its cognate *btaR2* (yellow) are outlined. BtaK and BtaN are multi-domain NRPS enzymes with the domain organizations shown. (C) HPLC-MS comparison of wt E264 (red and blue traces) with *btaK::Tn* (black and gray traces) in the presence of Tmp. Extracted are peaks corresponding to **29** (gray and blue) or **30** (black and red). The *btaK* mutant fails to produce any of the acybolins. (D) HPLC-Qtof-MS analysis of *ΔbtaI1/I2/I3* triple mutant in the presence of only Tmp (black trace), only 3-OH-C_{10}-HSL (gray), both Tmp and 3-OH-C_{10}-HSL (red), both Tmp and 3-OH-C_8-HSL (blue), or Tmp, 3-OH-C_{10}-HSL and 3-OH-C_8-HSL (green). Each trace is extracted for acybolin A (**29**). Both Tmp and AHL are required for production of any acybolins in this mutant. The traces in (C) and (D) are offset in both axes for clarity.